

# Simultaneous Force and Temperature Measurement Using Optical Microfiber Asymmetrical Interferometer

Caibin YU<sup>1</sup>, Xiaoxiao CHEN<sup>2</sup>, Yuan GONG<sup>1\*</sup>, Yu WU<sup>1</sup>,  
Yunjiang RAO<sup>1</sup>, and Gangding PENG<sup>3</sup>

<sup>1</sup>Key Laboratory of Optical Fiber Sensing and Communications (Ministry of Education of China), University of Electronic Science and Technology of China, Chengdu, 611731, China

<sup>2</sup>National Institute of Measurement and Testing Technology, Chengdu, 610021, China

<sup>3</sup>School of Electrical Engineering and Telecommunications, University of New South Wales, Sydney, NSW 2052, Australia

\*Corresponding author: Yuan GONG      E-mail: ygong@uestc.edu.cn

**Abstract:** A novel optical microfiber asymmetric Fabry-Perot interferometric (MAFPI) sensor is developed for simultaneous measurement of force and temperature. The MAFPI structure is formed by a weak fiber Bragg grating (FBG), a section of the microfiber, and a cleaved fiber end surface. The narrowband beam reflected from the low-reflectivity FBG and the broadband beam from the Fresnel reflection interfere lead to its unique sensing performance. The force sensing is performed by detecting the bending-loss induced fringe contrast changes, while the Bragg wavelength shift is employed for temperature measurement. Sensitivities of 9.8 pm/°C and 0.025 dB/μN were obtained experimentally for temperature and force measurements, respectively.

**Keywords:** Optical microfiber, weak FBG, interferometric

---

Citation: Caibin YU, Xiaoxiao CHEN, Yuan GONG, Yu WU, Yunjiang RAO, and Gangding PENG, "Simultaneous Force and Temperature Measurement Using Optical Microfiber Asymmetrical Interferometer," *Photonic Sensors*, 2014, 4(3): 242–247.

---

## 1. Introduction

Since its first development [1], the optical micro/nanofiber [2] has been used as a platform for fiber-optic sensing [3, 4] and also for developing new passive components [5]. It has distinct advantages for sensing such as the high sensitivity due to its quite small diameter and strong evanescent wave [6] and quick response to the ambient parameter changes [7]. In the last decade, great efforts have been made to develop optical resonators or interferometers for sensing based on the optical microfiber. Various micro structures, like the micro-knot resonator [7, 8], micro-loop resonator [9],

micro Mach-Zehnder (MZ) interferometer [10], and micro Fabry-Perot (FP) interferometer [11], were developed with distinct sensing features. Further, a novel type of the optical microfiber sensing technology, called the microfiber coil [12–14], was developed to further enhance the sensitivity of sensing. However, multi-point sensing is relatively difficult for these sensors.

On the other hand, the microfiber Bragg grating (MFBG) has been extensively investigated recently. It perfectly combines the unique multiplexing capability of the fiber Bragg grating (FBG) with the high sensitivity feature of the optical microfiber.

---

Received: 21 April 2014 / Revised version: 11 June 2014

© The Author(s) 2014. This article is published with open access at Springerlink.com

DOI: 10.1007/s13320-014-0201-4

Article type: Regular

Various micromachining technologies have been used to fabricate such an MFBG, including focused ion beam milling [15, 16], 193-nm ArF excimer laser inscription [17, 18], and femtosecond laser micromachining [19]. Fiber-optic FP interferometers are also formed by symmetrical MFBGs [20]. In prior to the fabrication process of MFBGs, the pre-fabricated optical microfiber is easy to break, and the precise alignment of the microfiber and the laser beam for micromachining is essential, making the fabrication slow and cost-ineffective. Similar to the FBG, MFBG also suffers from the cross-sensitivity problem as both changes in the ambient temperature and the measurand contribute to the Bragg wavelength shift.

In this paper, a novel optical microfiber asymmetric Fabry-Perot interferometric sensor (MAFPI) is developed for simultaneous measurement of force and temperature. In our experiment, the MAFPI structure was based on a weak, tapered FBG and a cleaved fiber end. Compared with the fabrication process of the FP interferometer based on MFBG pairs [20], it is much more efficient to fabricate an FBG in the single mode fiber (SMF) firstly and then form a microfiber interferometer by the taper-drawing method [21, 22]. Dual parameter measurement was obtained through simultaneously detecting the fringe contrast and the peak wavelength of the interference spectra of the fiber microstructure. The force sensitivity is high due to the small diameter of the optical microfiber. It also has the great potential for mass multiplexing as the interference spectrum is dominated by the reflective spectrum of the weak, tapered FBG.

## 2. Fabrication and principle of MAFPI

The experimental setup for the fabrication of the MAFPI structure is schematically shown in Fig. 1. A low-reflectivity (LR-) FBG is first inscribed in a hydrogen-loaded single mode fiber (SMF) using a 248-nm KrF excimer laser as well as a phase mask. The laser beam transmitted through the phase mask

is spatially filtered to be 3 mm, inducing a short FBG. A pulse energy of 6.5 mJ and totally 700 pulses are used to fabricate an LR-FBG with a reflectivity as low as 3% – 4.5%. The pigtailed of the LR-FBG are fixed to a static translation stage and a one-dimensional (1-D) motorized translation stage, respectively, via two fiber holders. One end of the LR-FBG is heated by a hydrogen flame, and at the same time, the one-dimensional motorized translation stage is controlled to stretch the pigtail into an optical microfiber. The LR-FBG is located besides the end of the microfiber, whose far end with a diameter of 125  $\mu\text{m}$  is cleaved to obtain the Fresnel reflection. In our experiment, the taper length was about 20 mm controlled by the displacement of the 1-D motorized translation stage.

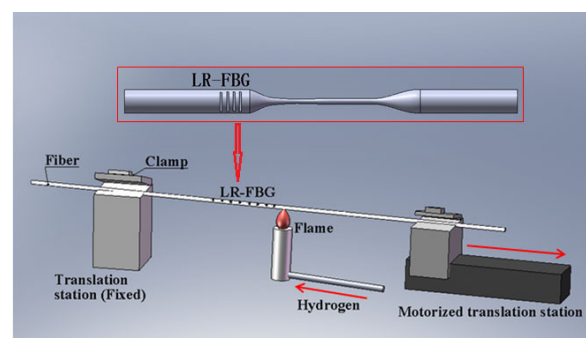


Fig. 1 Schematic diagram of the experimental setup for the fabrication of the MAFPI structure.

The structure is illustrated in the inset of Fig. 1. The MAFPI structure consists of an LR-FBG, a section of the optical microfiber, and a fiber end surface with Fresnel-reflection. The reflective spectra of the MAFPI structure are measured by a wavelength-swept-laser-based optical spectrum analyzer (OSA, Agilent) via a 50:50 fiber coupler, as shown in Fig. 2(a). In order to measure both temperature and force responses, we fix the LR-FBG by gluing it to a glass substrate and put it horizontally. In this case, the force-induced Bragg wavelength shift is eliminated. The gluing point is just between the LR-FBG and the optical microfiber and will not lead to the additional transmission loss. The microfiber is naturally bent by the gravity of the residual 125  $\mu\text{m}$ -SMF, as shown in Fig. 2(b). A mass

with the uniform density in the longitudinal direction is employed to calibrate the force response of the MAFPI sensor. It is adhered to the 125  $\mu\text{m}$ -SMF section between the microfiber and the Fresnel end surface. This will influence neither the transmission loss of the microfiber nor the Fresnel reflection of the fiber end. Each time the force is changed slightly by cutting a small section of the long-shaped mass, and then the reduced weight is measured with an accuracy of 0.0001 g by an analytical balance.

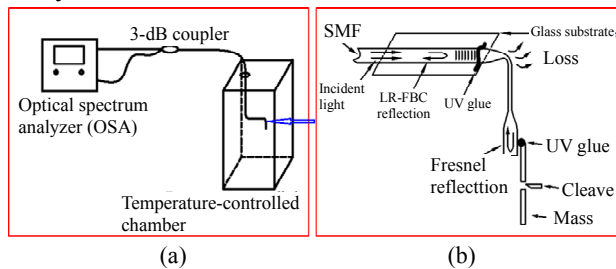


Fig. 2 Schematic setup of (a) temperature sensing and (b) force sensing experiments.

The mechanism of the MAFPI sensor can be simplified as a two-beam interference model and is described as follows. The interference spectrum of the MAFPI sensor in the Bragg wavelength range is formed by the LR-FBG reflected light, and the Fresnel reflected light can be expressed as

$$I(\lambda) = I_{\text{FBG}}(\lambda) + I_{\text{Fresnel}}(\lambda) + 2\sqrt{I_{\text{FBG}}(\lambda)I_{\text{Fresnel}}(\lambda)}\cos\varphi \quad (2)$$

where  $I_{\text{FBG}}(\lambda)$  and  $I_{\text{Fresnel}}(\lambda)$  are the reflective intensities of the LR-FBG and the Fresnel end surface, respectively. The FBG has a narrowband reflection, while the fiber end surface has a broadband Fresnel reflection.

This asymmetrical structure leads to a unique performance of the MAFPI sensor compared with two symmetrical interferometric structures. One is based on two Fresnel reflections, known as the extrinsic fiber-optic Fabry-Perot interferometer (EFPI) [23]. The other is the FBG-pair-based fiber-optic Fabry-Perot interferometer (FBG-FPI) [24]. In the EFPI, two broadband reflective beams interfere, and the fringes cover a wide range in the wavelength domain ( $>100$  nm). The wavelength

division multiplexing (WDM) becomes invalid. Therefore, spatial frequency multiplexing (SFM) is often employed by using EFPIs with different cavity lengths [25]. However, the number of sensors multiplexed by the SFM method is limited. As the cavity length increases, the propagation loss of light in the cavity increases, making the fringe contrast degrade and indicating a maximum cavity length. And for the fabrication of an FBG-FPI, it is requested that the narrow reflective band, generally with a 3-dB bandwidth of 0.2 nm – 0.3 nm, of the two FBGs should be exactly overlapped [24]. Further, the Bragg wavelengths of the two FBGs should change synchronously during the sensing process. If either of the two above requirements is broken, the interference fringes will degrade or even disappear.

### 3. Sensing experiment and discussion

In the temperature sensing experiment, the MAFPI sensor was placed in a chamber with temperature controlled from 20  $^{\circ}\text{C}$  to 110  $^{\circ}\text{C}$  with an interval of 15  $^{\circ}\text{C}$ . The reflective spectra were recorded by the OSA, as shown in Fig. 3(a). A red shift of the Bragg reflective spectrum was clearly observed. By fitting the envelope of the Bragg reflective spectrum to a Gaussian function, the Bragg wavelength was determined. To clarify the Bragg wavelength shift, the Gaussian fits are shown in Fig. 3(b). In our experiment, the applied force was isolated from the FBG by the ultraviolet (UV) glue. Thus, the Bragg wavelength shift,  $\Delta\lambda_B / \lambda_B = (\xi + \alpha)\Delta T$  is originated from the thermo-optic and the elasto-optic effects, i.e., the thermal- and stress-induced refractive index changes of the fiber.  $\xi$  and  $\alpha$  are thermo-optic coefficient and elasto-optic coefficient, respectively.

The LR-FBG is responsible for the temperature sensing, duo to the interferometric structure for the force sensing. In the force sensing experiment, a mass with the uniform density in the longitudinal direction was employed to calibrate the force response of the MAFPI sensor. Each time the

external force decreases slightly by cutting a small section of the long-shaped mass, the radius of curvature of the bent microfiber increases, and accordingly, the bending loss is reduced. According to the two-beam interference model, the fringe contrast of the inference spectrum increases as the reflectivities of the two reflective surfaces get closer.

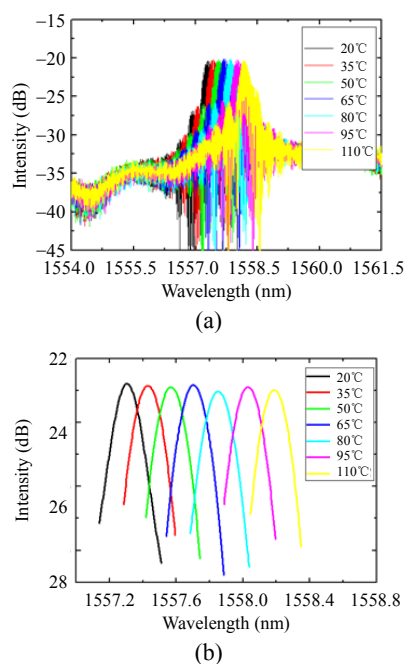


Fig. 3 Reflective spectra of the sensor under different temperatures: (a) reflective spectra of the MAFPI sensor and (b) Bragg wavelength shift at different temperatures.

The interference spectra of the MAFPI structure are shown in Fig. 4(a). The spectrum near the Bragg wavelength is enlarged and shown as a function of the external force changes in Fig. 4(b). It is indicated by the experimental results that the fringe contrast of the interference spectra increases as the force decreases. Although an interference fringe shift of about tens of picometers is observed from Fig. 4(b) during the force sensing experiment, the Bragg wavelength do not shift with the external force, which is confirmed by fitting the reflective spectra in Fig. 4(a) with the Gaussian function and detecting the Bragg wavelength.

The Bragg wavelength shift as a function of the external temperature and force changes is shown in Fig. 5(a), with solid circles and void squares, respectively. The Bragg wavelength shift has a good

linear relation to the temperature changes, while the shift is insensitive to the force variations. The temperature sensitivity is statistically determined to be  $9.8 \pm 0.1 \text{ pm}/^\circ\text{C}$ .

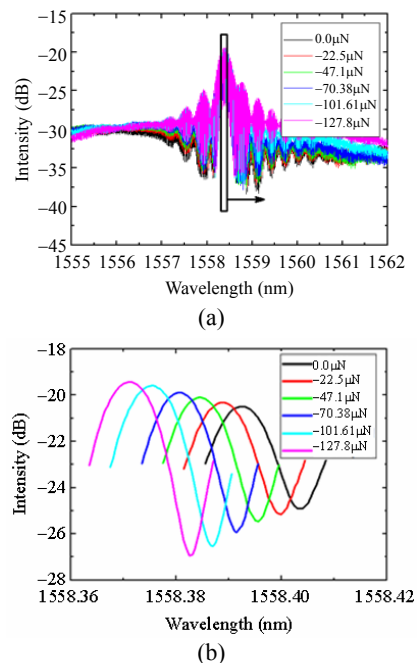


Fig. 4 Reflective spectra of the sensor under different external force: (a) reflective spectra of the MAFPI sensor and (b) interference fringes near the Bragg wavelength under different external forces.

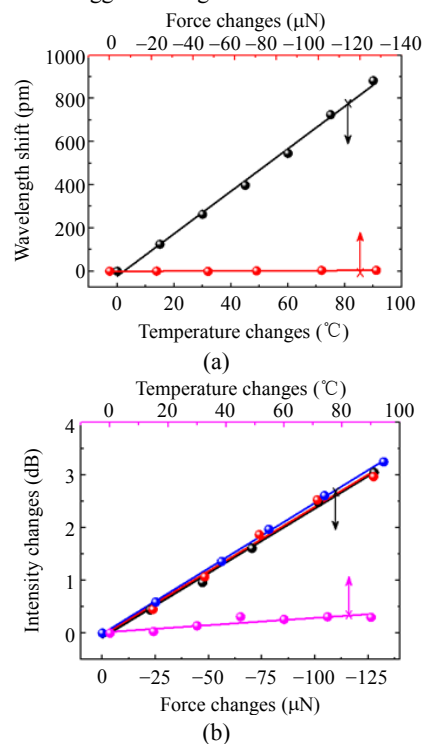


Fig. 5 Sensing performance of the sensors: (a) Bragg wavelength shift and (b) interference fringe contrast as functions of temperature and force changes.

The fringe contrast of the interference spectrum as a function of external force and temperature changes is shown in Fig. 5(b), with solid circles and void squares, respectively. Good linearity is obtained. The range of the force measurement is controlled within several hundreds of micro-Newtons. There are several applications for the force sensor in this scale [26]. The force sensitivity is 0.025 dB/ $\mu\text{N}$ , while the temperature sensitivity is 0.004 dB/ $^{\circ}\text{C}$ . Therefore, the cross sensitivity of the temperature and force is 0.16  $\mu\text{N}/^{\circ}\text{C}$  without temperature compensation. In some cases, this cross sensitivity can be negligible. For the precise measurement of force, temperature compensation is necessary. The temperature changes can be determined by measuring the Bragg wavelength shift, and the temperature-induced fringe contrast change should be subtracted from the whole contrast change. For the dual parameter measurement, a  $2 \times 2$  coefficient matrix can be used [27].

In summary, we developed a fiber-optic sensor for simultaneous measurement of force and temperature. The structure was based on a weak FBG, a section of the bent microfiber, and a fiber end surface with Fresnel reflection. It has the advantages of easy-to-fabricate, low cost, and also has the potential for mass multiplexing capacity by combining the wavelength division multiplexing (WDM) and spatial frequency multiplexing (SFM) methods.

## Acknowledgment

This work is supported by the National Natural Science Foundation of China (61107073, 61107072 and 61290312), Fundamental Research Funds for the Central Universities (ZYGX2011J002), Research Fund for the Doctoral Program of Higher Education of China (20110185120020), Program for Changjiang Scholars and Innovative Research Team in University (PCSIRT, IRT1218), and the 111 Project (B14039).

**Open Access** This article is distributed under the terms of the Creative Commons Attribution License which permits any use, distribution, and reproduction in any medium, provided the original author(s) and source are credited.

## References

- [1] L. M. Tong, R. R. Gattass, J. B. Ashcomv, S. L. He, J. Y. Lou, M. Y. Shen, *et al.*, "Subwavelength-diameter silica wires for low-loss optical wave guiding," *Nature*, 2003, 426(6968): 816–819.
- [2] G. Brambilla, "Optical fiber nanowires and microwires: a review," *Journal of Optics*, 2010, 12(4): 043001.
- [3] J. Scheuer and M. Sumetsky, "Trap-door optical buffering using a flat-top coupled microring filter: the superluminal cavity approach," *Optics Letters*, 2013, 38(18): 3534–3537.
- [4] L. Zhang, J. Y. Lou, and L. M. Tong, "Polymer single-nanowire optical sensors," *Photonic Sensors*, 2011, 1(1): 31–42.
- [5] R. Ismaeel, T. Lee, M. Ding, M. Belal, and G. Brambilla, "Optical microfiber passive components," *Laser and Photonics Reviews*, 2013, 7(3): 350–384.
- [6] F. X. Gu, L. Zhang, X. F. Yin, and L. M. Tong, "Polymer single-nanowire optical sensors," *Nano Letters*, 2008, 8(9): 2757–2761.
- [7] Y. Wu, Y. J. Rao, Y. Chen, and Y. Gong, "Miniature fiber-optic temperature sensors based on silica/polymer microfiber knot resonators," *Optics Express*, 2009, 17(20): 18142–18147.
- [8] X. S. Jiang, L. M. Tong, G. Vienne, X. Guo, T. Albert, Q. Yang, and D. R. Yang, "Demonstration of optical microfiber knot resonators," *Applied Physics Letters*, 2006, 88(22): 223501.
- [9] M. Sumetsky, Y. Dulashko, J. M. Fini, and A. Hale, "Optical microfiber loop resonator," *Applied Physics Letters*, 2005, 86: 161108.
- [10] J. L. Kou, J. Feng, Q. J. Wang, F. Xu, and Y. Q. Lu, "Microfiber-probe-based ultrasmall interferometric sensor," *Optics Letters*, 2010, 35(13): 2308.
- [11] M. Sumetsky, "Fabrication and study of bent and coiled free silica nanowires: self-coupling microloop optical interferometer," *Optics Express*, 2004, 12(15): 3521–3531.
- [12] F. Xu, P. Horak, and G. Brambilla, "Optical microfiber coil resonator refractometric sensor," *Optics Express*, 2007, 15(12): 7888–7893.
- [13] F. Xu and G. Brambilla, "Demonstration of a refractometric sensor based on optical microfiber coil resonator," *Applied Physics Letters*, 2008, 92(10): 101126.
- [14] W. Luo, J. L. Kou, Y. Chen, F. Xu, and Y. Q. Lu,

- “Ultra-highly sensitive surface-corrugated microfiber Bragg grating force sensor,” *Applied Physics Letters*, 2012, 101(13): 133502.
- [15] Y. Liu, C. Meng, A. P. Zhang, Y. Xiao, H. Yu, and L. M. Tong, “Compact microfiber Bragg gratings with high-index contrast,” *Optics Letters*, 2011, 36(16), 3115–3117.
- [16] Y. Ran, Y. N. Tan, L. P. Sun, S. Gao, J. Li, L. Jin, *et al.*, “193 nm excimer laser inscribed Bragg gratings in microfibers for refractive index sensing,” *Optics Express*, 2011, 19(19): 18577–18583.
- [17] S. Gao, L. Jin, Y. Ran, L. P. Sun, J. Li, and B. O. Guan, “Temperature compensated microfiber Bragg gratings,” *Optics Express*, 2012, 20(16): 18281–18286.
- [18] X. Fang, C. R. Liao, and D. N. Wang, “Femtosecond laser fabricated fiber Bragg grating in microfiber for refractive index sensing,” *Optics Letters*, 2010, 35(7): 1007–1009.
- [19] J. Li, X. Shen, L. P. Sun, and B. O. Guan, “Characteristics of microfiber Fabry-Perot resonators fabricated by UV exposure,” *Optics Express*, 2013, 21(10): 12111–12121.
- [20] J. Zhang, Q. Sun, R. Liang, J. Wo, D. Liu, and P. Shum, “Microfiber Fabry-Perot interferometer fabricated by taper-drawing technique and its application as a radio frequency interrogated refractive index sensor,” *Optics Letters*, 2012, 37(14): 2925–2927.
- [21] Y. Gong, C. B. Yu, T. T. Wang, X. P. Liu, Y. Wu, Y. J. Rao, *et al.*, “Highly sensitive force sensor based on optical microfiber asymmetrical Fabry-Perot interferometer,” *Optics Express*, 2014, 22(3): 3578–3584.
- [22] T. Wei, Y. Han, Y. Li, H. Tsai, and H. Xiao, “Temperature-insensitive miniaturized fiber inline Fabry-Perot interferometer for highly sensitive refractive index measurement,” *Optics Express*, 2008, 16(8): 5764.
- [23] Y. O. Barmenkov, D. Zalvidea, S. Torres-Peiró, J. L. Cruz, and M. V. Andrés, “Effective length of short Fabry-Perot cavity formed by uniform fiber Bragg gratings,” *Optics Express*, 2006, 14(14): 6394–6399.
- [24] Y. J. Rao, “Recent progress in fiber-optic extrinsic Fabry-Perot interferometric sensors,” *Optical Fiber Technology*, 2006, 12(3): 227–237.
- [25] Y. Fujii, “Method of generating and measuring static small force using down-slope component of gravity,” *Review of Scientific Instruments*, 2007, 78(6): 066104.
- [26] F. Xie, X. F. Chen, L. Zhang, and M. Song, “Multi-parameter and multi-functional fiber grating sensing technology,” *Optics Laser Engineering*, 2006, 44: 1088.